

# Universal large-scale entanglement in two-dimensional gapless systems

Hyejin Ju,<sup>1</sup> Ann B. Kallin,<sup>2</sup> Paul Fendley,<sup>3,4</sup> Matthew B. Hastings,<sup>4</sup> and Roger G. Melko<sup>2</sup>

<sup>1</sup>*Department of Physics, University of California, Santa Barbara, CA, 93106-9530*

<sup>2</sup>*Department of Physics and Astronomy, University of Waterloo, Ontario, N2L 3G1, Canada*

<sup>3</sup>*Physics Department, University of Virginia, Charlottesville, VA 22904-4714*

<sup>4</sup>*Microsoft Research, Station Q, CNSI Building, University of California, Santa Barbara, CA, 93106-9530*

(Dated: July 19, 2022)

We numerically determine universal terms in the ground-state entanglement entropy of several two dimensional (2D) gapless systems, including a Heisenberg model with Néel order, a free Dirac fermion in the  $\pi$ -flux phase, and the nearest-neighbor resonating-valence bond wave function. For these models, we show that the entanglement entropy between cylindrical regions of length  $x$  and  $L - x$ , extending around a torus of length  $L$ , depends upon the dimensionless ratio  $x/L$ . This can be well-approximated on finite-size lattices by a function  $\ln(\sin(\pi x/L))$  akin to the familiar chord-length dependence in one dimension. We provide evidence, however, that the precise form of this bulk-dependent contribution is a more general universal function in the 2D thermodynamic limit.

*Introduction*— The study of quantum condensed matter systems is benefiting from an infusion of ideas related to quantum information and entanglement. The importance of this new resource is strikingly demonstrated in the study of entanglement entropy at one-dimensional (1D) quantum critical points with conformal invariance. Conformal field theory (CFT) provides an important universal number, the *central charge*  $c$ , that appears in an astonishing array of physical quantities [1]. A given CFT, and thus any quantum critical points it describes, can be characterized by this number. Its numerical or analytical determination provides an invaluable tool in identifying which, if any, CFT describes the scaling limit of a given Hamiltonian. Computing the entanglement entropy has proved a very useful way of finding  $c$  numerically. It can be extracted directly from the ground-state wavefunction by measuring its Renyi entanglement entropy,  $S_n = 1/(1-n) \ln [\text{Tr} \rho_A^n]$ , where region  $A$  is entangled with its complement, region  $B$ . Namely, in a system with total length  $L$  and the region  $A$  being of length  $x$ , the scaling of the Renyi entropy in 1D critical systems depends on the “chord length” as [2–5],

$$S_n = \frac{c}{6} \left(1 + \frac{1}{n}\right) \ln \left[ \frac{L}{\pi} \sin \left( \frac{\pi x}{L} \right) \right], \quad (1)$$

with the central charge appearing as the coefficient.

In higher dimensions, the scaling behavior of the entanglement entropy is much less well-understood. Ground states of local Hamiltonians are generally believed to produce an “area-law” (i.e. boundary) scaling [6], the subleading corrections to which may be universal quantities that can be used to identify and characterize quantum phases and phase transitions. A well established example of such is the topological entanglement entropy [7–10] of a gapped state with topological order. In gapless states, the subleading corrections may still potentially harbor universal quantities. It is conceivable that such quantities could be used to define an “effective” central charge in two spatial dimensions, but there are strong

constraints on any proposal [11]. The best-understood gapless situation in two dimensions is the special case of a conformal quantum critical point, where the ground state itself is written in terms of a two-dimensional (2D) CFT [12–18]. In the presence of a spontaneously broken continuous symmetry, Goldstone modes produce a subleading bulk logarithmic correction [19, 20]. Subleading logarithms from corner contributions with universal coefficients also occur at some critical points [14, 21, 22].

The purpose of this paper is to analyze one type of universal term occurring in 2D gapless systems. Gapless modes typically have long-range correlations, so it is possible for the entanglement entropy to depend on the size and shape of the regions  $A$  and  $B$ . Indeed, the 1D result (1) is manifestly size-dependent. We show how similar behavior also occurs in 2D.

We study the finite-size scaling of the second Renyi entropy for the ground states of several two-dimensional gapless systems on the square lattice using quantum Monte Carlo (QMC) simulations. It is possible to vary the size of regions  $A$  and  $B$  without changing the length of the boundary between in a toroidal lattice geometry, where  $A$  and  $B$  are cylinders as in Fig. 1. We examine the Néel ground state of the Heisenberg model, and the nearest-neighbor resonating-valence-bond (RVB) wavefunction, in this geometry. In both cases, we find a size- and shape-dependent scaling function that closely mimics the chord-length contribution in 1D in Eq. (1).

To probe this behavior in a simpler system, we also study free spinless fermions in the  $\pi$ -flux phase and find that the entanglement scaling also has a universal size- and shape-dependent piece. For finite-size systems, this closely mimics the chord length, but in the infinite-size limit we observe it to cross over to a different non-trivial function. Among other consequences, this term will give a non-zero signature in the entanglement quantities [9, 10] designed to look for topological order, which complicates any possible generalization of the topological entanglement entropy to gapless spin-liquid states.

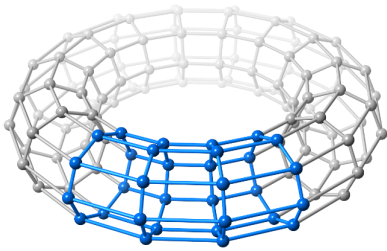


FIG. 1: An  $8 \times 16$  toroidal lattice. The width of cylindrical region  $A$  (blue) is  $x = 4$ . The boundary length between region  $A$  and its complement is  $\ell = 16$ .

*Fermions with  $\pi$ -flux*— We begin by considering free spinless fermions on a square lattice, with  $\pi$ -flux through each plaquette. We consider a torus of size  $L_x$  by  $L_y$ , and measure the entanglement using a cornerless cylindrical region  $A$  (Fig. 1) with a constant boundary length  $\ell = 2L_y$ . We denote the width of region  $A$  by  $x$ . This system has Dirac points near momentum  $k_y = 0$  and  $k_y = \pi$ . We take anti-periodic boundary conditions in the  $x$ -direction so that there will be no exact zero mode. We use exact numerical diagonalization of the single-particle Hamiltonian to compute the entropy.

The entanglement entropy of 2+1-dimensional conformally invariant systems such as this has been argued to be of the form [23, 24],

$$S_n \sim \text{const.} \times \ell/a + \gamma(x/L_x, L_y/L_x), \quad (2)$$

where  $\gamma$  is a universal scaling function of the dimensionless ratios. The area-law term proportional to the boundary length  $\ell$  depends on the lattice constant  $a$ , and so the constant is non-universal. A crucial difference from the result in 1D, Eq. (1), is that  $a$  only appears in the area law term. In contrast, the one-dimensional result can be written as a sum of two terms as  $S_n = C \ln[\sin(\frac{\pi x}{L})] + C \ln[\frac{L}{\pi}]$ , where  $C = c/6(1 + 1/n)$ . The first term is a universal function of the dimensionless ratio  $x/L$ , akin to the function  $\gamma$  above, while the second term involves the lattice scale, as it diverges with  $L$ .

To illustrate the absence of such an “additive logarithm” (a logarithmic divergence depending on  $L/a$ ) in 2D, we treat this free system as a collection of independent systems in 1D labeled by the momenta  $k_y$ . The  $k_y = 0$  mode contributes an additive logarithm  $C \ln(L_x)$  to the entropy, while the modes with small  $k_y \neq 0$  contribute additive logarithms  $C \ln(k_y^{-1})$  [2, 4, 5]. Summing over  $k_y = 2\pi j/L_y$ , this gives an entropy  $C[\ln(L_x) + 2 \sum_{j=1}^{j \sim L_y} \ln(L_y/2\pi j)] = C \ln(L_x) + 2C \ln[(L_y/2\pi)^{L_y/L_y}]$ , where the factor of 2 arises from summing over positive and negative  $m \neq 0$ . Using Stirling’s formula for  $L_y!$ , one finds that the additive logarithm terms add to  $C[\ln(L_x) - \ln(L_y)] = C \ln(L_x/L_y)$ . This can be absorbed into the scaling function  $\gamma$ , so that

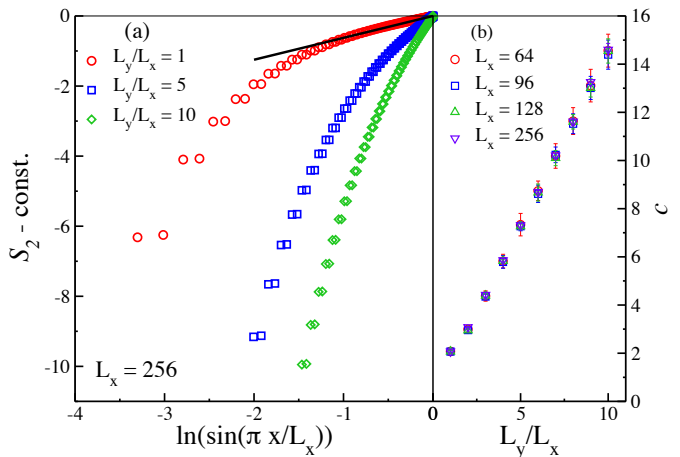


FIG. 2: (a) Renyi entropy of  $L_x = 256$  Dirac fermion model, with an arbitrary constant subtracted off each data set. The straight line is Eq. (1) plotted with  $c = 2$ . It is clear that deviations from linearity increase for larger  $L_y/L_x$ . (b) A set of points near  $x = 0$  is shown to follow the 1D result  $\ln(\sin(\pi x/L_x))$ . Notice that the “central charge”,  $c$ , in this region is system-size independent.

there is no additive logarithm. A more precise calculation would include the effect of finite  $L_x$ , but we ignore this since it does not affect the cancellation of additive logarithms. A similar calculation near  $k_y = \pi$  leads to a cancellation of the additive logarithm there.

The entropy of a given  $k_y$  mode contains, in addition to the additive logarithmic divergence in  $k_y$ , a universal scaling function  $G(x/L_x, k_y x)$ . At  $k_y = 0$ , we see the chord-length scaling  $C \ln[\sin(\frac{\pi x}{L})]$  (Fig. 2), but for  $k_y \neq 0$  and for  $k_y x$  large, the chord-length scaling disappears and the entropy becomes roughly flat as a function of  $x/L$ . In fact, for  $L_y = L_x = L$ , the lowest  $k_y$  mode has a mass  $2k_y = 4\pi/L$ . This factor of  $4\pi \approx 13$  means this mass is rather large, and so the entropy of this mode is flat for a large range of  $x/L$ . As a result, for  $L_y = L_x = L$ , the entropy of the 2D system appears to display 1D chord length scaling over a wide range of  $x/L_x$ .

*Quantum Monte Carlo*— Using QMC techniques we simulate both the Heisenberg ground state and the RVB wavefunction in 2D. The Heisenberg ground state is projected from a trial state by applying a high power of the Hamiltonian,  $H = \sum_{\langle ij \rangle} \mathbf{S}_i \cdot \mathbf{S}_j$ , via a QMC method operating in the valence bond (VB) basis [25]. The RVB wavefunction is an equal-amplitude superposition  $|\Psi\rangle = \sum_{\alpha} |V_{\alpha}\rangle$  of all nearest-neighbor valence-bond states,

$$|V_{\alpha}\rangle = \frac{1}{2^{N/4}} \prod_{i=1}^{N/2} (|\uparrow_i \downarrow_{j_{\alpha}}\rangle - |\downarrow_i \uparrow_{j_{\alpha}}\rangle), \quad (3)$$

defined by requiring that each spin  $i$  on one sublattice be in a singlet with one of its nearest neighbors  $j_{\alpha}$  [26, 27].

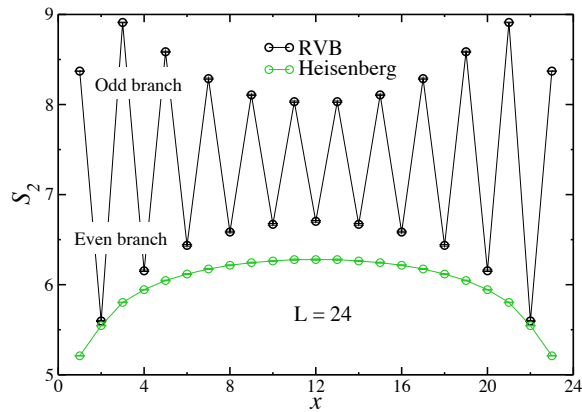


FIG. 3: The second Renyi entropy for the Néel and RVB states for  $L = 24$ . Note that the entanglement entropy for the RVB splits into two branches, even and odd, which may be related to the existence of topological sectors in the underlying transition graphs.

The RVB Monte Carlo sampling algorithm does a random walk through the possible states by creating a defect at some spatial point and propagating it through the system (thereby rearranging the nearest-neighbor bonds) until the defect reaches the initial point and its path forms a closed loop [28]. If we visualize the Heisenberg ground state in this VB language, then the RVB wavefunction is its largest component, the remainder of the state being superpositions of longer bonds, decaying with their length as  $1/r^3$  [25]. Likewise, the RVB wavefunction is the ground state of a local (but longer-range) Hamiltonian that includes a Heisenberg term [29].

We consider the same geometry as for the  $\pi$ -flux fermions, with  $L_x = L_y = L$  (see Fig. 1). In Fig. 3, we plot QMC results for the second Renyi entropy in the Néel and RVB states on a  $24 \times 24$  torus. Several features of the entanglement scaling are clear from this plot. First, note that the data for the Néel state has a significant curvature as a function of  $x$ . This curvature was first seen in Ref. [19] but not explored in detail (instead, using a fixed  $x/L$  a surprising subleading logarithmic term  $\propto \ln(\ell)$  was found). The entropy of the RVB wave function exhibits an obvious dependence on whether  $x$  is even or odd which we discuss in more detail below. In each of the even and odd “branches”, there is significant curvature in the  $x$  dependence as with the Heisenberg case.

To capture the  $x$ -dependent curvature of these wavefunctions, we fit the data with the scaling ansatz,

$$S_2 = a\ell + b \ln(\ell) + c(L) \ln \left[ \sin \left( \frac{\pi x}{L} \right) \right] + d, \quad (4)$$

motivated by the chord length in Eq. (1). We begin by examining the Néel state in Fig. 4. For a fixed linear system size  $L$  and boundary length  $\ell$ , plots of  $S_2$  versus

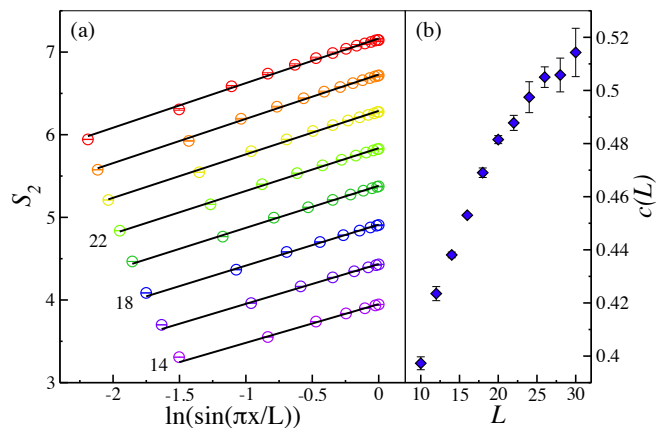


FIG. 4: (a) Heisenberg data and linear fits (excluding the first two data points on the left) for  $L = 14, 16, \dots, 28$  plotted in terms of the log of the “chord-length”,  $\ln \left[ \sin \frac{\pi x}{L} \right]$ . (b) Slopes of the fits,  $c(L)$ , exhibit a strong dependence on the system size,  $L$ .

$\ln \left[ \sin \left( \frac{\pi x}{L} \right) \right]$  would yield a straight line if Eq. (4) were obeyed perfectly. The plots indeed are quite close to straight lines for a fixed  $L$ .

The second Renyi entropy therefore displays at the very least an effective chord-length dependence over a large range of  $x$  for the square torus. It is possible that the apparent chord-length scaling of this 2D system is not perfectly obeyed in the thermodynamic limit, and that this fact is manifest in slight deviations from straight-line behavior in Fig. 4(a). This would be a similar scenario to the deviation from chord-length scaling observed for  $\pi$ -flux fermions in Fig. 2. However, it is difficult to draw a firm conclusion regarding the statistical significance of any deviation from Eq. (4) scaling in our present data, due to limited system sizes and stochastic error.

We can however further examine the deviation from conformal-style scaling by examining the universality of the coefficient of the chord-length in the Néel state. To do this, we extract the  $L$ -dependence of the coefficient  $c(L)$  in Eq. (4). As illustrated in Fig. 4(b), the coefficient does not approach a constant for the system sizes that we have studied, but rather has some functional dependence on  $L$ . This functional dependence is apparently sub-linear. It is interesting to speculate that  $c(L) \sim L^p$  with  $p \leq 1$ . A rigorous analysis of the data along these lines is impossible however within the current accuracy of our QMC simulations.

We next examine the scaling of the Renyi entropy in the RVB wavefunction. As seen in Fig. 3, a striking two-branch structure exists, depending on whether the distance  $x$  is even or odd. The presence of the two branches presumably is related to the fact that correlators in the RVB state have a pronounced even-odd dependence. Moreover, simple counting arguments of prototyp-

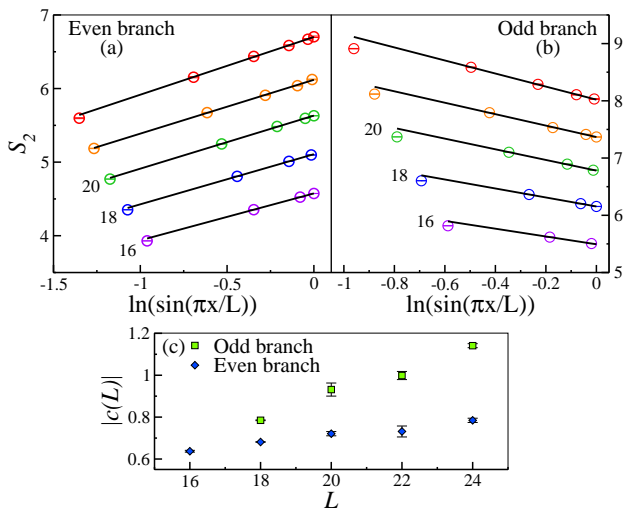


FIG. 5: (a) Even and (b) odd branches of the second Renyi entropy plotted against the log of the “chord-length”. We exclude  $x = 1, 2$  data from the plots, as there is some crossover behavior observed in Fig. 3. (c) The absolute value of the slopes,  $|c(L)|$ , as a function of the system size,  $L$ . As with the Heisenberg, there is a strong dependence on  $L$ .

ical valence-bond configurations in the  $(0,0)$  topological sector [26, 27] show that the number of valence bonds crossing from region  $A$  to region  $B$  alternates strongly with  $x$ . This  $L = 24$  data displays a clear  $x$ -dependent curvature in each branch. This can be analyzed more closely by attempting fits of the form Eq. (4) to each branch individually. From Fig. 5(a) and (b), it is clear that fits to the scaling ansatz to both branches are quite accurate when the extremal values of  $x$  are excluded. It is worth noting that in the closely related quantum dimer model on the square lattice, no such term appears: in this geometry, the only subleading term in the entanglement entropy is constant [12, 13, 15–18].

We can attempt to extract the size dependence of the coefficient  $c$  in a similar manner as for Heisenberg. Unfortunately, due to the two-branch structure, each curve on this plot has essentially half the usable data compared to the analogous Heisenberg results in Fig. 4. Nonetheless, the result (Fig. 5(c)) shows that a significant  $L$ -dependence seems to exist in the RVB wavefunction as well. This again suggests that, although the fit to a chord-length scaling at fixed  $L$  is consistent within the accuracy of our data, subtle corrections to this form may come into play in the 2D thermodynamic limit.

*Discussion*— We have studied the Renyi entanglement entropy in the ground state of three gapless systems on  $L_x \times L_y$  toroidal lattices, where the subregion  $A$  is a cylinder of length  $x$ . We have demonstrated that it contains a universal subleading scaling term  $\gamma(x/L_x, L_y/L_x)$ , which depends on bulk quantities, namely the dimensionless aspect ratios of the sub-

region and the lattice linear dimensions. Note that while numerical measurement of topological entanglement entropy [9, 10] has been used to probe topological properties of *gapped* phases [30], the universal subleading term considered here means that a measurement of topological entanglement entropy in a *gapless* phase could give either a zero or non-zero result, even without any topological aspects of the phase (though measurements in the  $U(1)$  superfluid phase yielded a vanishing number [30]). Interestingly, just as strong sub-additivity constrains the sign of the Levin-Wen entropy [10], it also implies, for fixed  $L_x, L_y$ , that  $\gamma$  for the von Neumann entropy is a concave-down function of  $x$ .

Our quantum Monte Carlo simulations of the Heisenberg Néel ground state and the short-range RVB wavefunction with  $L_x = L_y = L$  show an almost-perfect logarithmic dependence of  $\gamma$  on the chord length  $\sin(\pi x/L)$ . It appears that the coefficient of this term is not a universal constant, however, which might suggest that care must be taken in the order of limits with which the thermodynamic limit is approached. A study of the crossover from one to two dimensions might illuminate this issue further. Further evidence that the true 2D scaling function might not be exactly the chord-length form is given by the scaling of gapless Dirac fermions in the  $\pi$ -flux phase. Here we have argued that such scaling is superseded by a sum over transverse modes, leading to a different (unknown) functional form in 2D. Furthermore, spontaneous symmetry breaking in the Heisenberg model may complicate measurement of the entanglement entropy. The fact that a complete characterization of the scaling behavior in the Néel and RVB states remains a challenge, despite the large lattice sizes studied to date, underlines the absolute necessity for using large-scale QMC simulations for the study of entanglement entropy.

Regardless of the precise functional form of  $\gamma(x/L_x, L_y/L_x)$ , its general existence in gapless wavefunctions in 2D would have some profound consequences. Besides the immediate complications in attempting to use entanglement as a probe to detect gapless spin liquids mentioned above, the similarity of the scaling function to a chord-length (present in 1D conformally invariant systems) raises the tantalizing possibility that our results will prove useful in characterizing higher-dimensional critical points. Indeed, since the search for a  $c$ -theorem [31] valid in higher dimensions is of intense interest across several disparate fields of physics (see e.g. [23, 32–34]), we hope our results will inspire a broader examination of this scaling term in 2D gapless states.

*Acknowledgments*— The authors thank A. Del Maestro, E. Fradkin, I. Klich, K. Intriligator, M. Metlitski, E.G. Moon, R. Myers and A. Sandvik for enlightening discussions. R.G.M. would like to acknowledge the support of Microsoft Station Q for hospitality during a visit. This work has been supported by the Natural Sciences and Engineering Research Council of Canada (NSERC),

and by the US NSF via grants DMR/MPS-0704666 and DMR/MPS1006549. Simulations were performed on the computing facilities of SHARCNET.

- 
- [1] J. Cardy, *J. Stat. Mech.: Theor. Exp.* **2010**, P10004 (2010).
- [2] C. Holzhey, F. Larsen, and F. Wilczek, *Nucl. Phys. B* **424**, 443 (1994).
- [3] G. Vidal, J. I. Latorre, E. Rico, and A. Kitaev, *Phys. Rev. Lett.* **90**, 227902 (2003).
- [4] V. E. Korepin, *Phys. Rev. Lett.* **92**, 096402 (2004).
- [5] P. Calabrese and J. Cardy, *J. Stat. Mech.: Theor. Exp.* **P06002** (2004).
- [6] J. Eisert, M. Cramer, and M. B. Plenio, *Rev. Mod. Phys.* **82**, 277 (2010).
- [7] A. Hamma, R. Ionicioiu, and P. Zanardi, *Phys. Lett. A* **337**, 22 (2005).
- [8] A. Hamma, R. Ionicioiu, and P. Zanardi, *Phys. Rev. A* **71**, 022315 (2005).
- [9] A. Kitaev and J. Preskill, *Phys. Rev. Lett.* **96**, 110404 (2006).
- [10] M. Levin and X.-G. Wen, *Phys. Rev. Lett* **96**, 110405 (2006).
- [11] P. Calabrese and J. Cardy, *J. Phys. A: Mathematical and Theoretical* **42**, 504005 (2009).
- [12] J.-M. Stéphan, S. Furukawa, G. Misguich, and V. Pasquier, *Phys. Rev. B* **80**, 184421 (2009).
- [13] B. Hsu, M. Mulligan, E. Fradkin, and E.-A. Kim, *Phys. Rev. B* **79**, 115421 (2009).
- [14] E. Fradkin and J. Moore, *Phys. Rev. Lett* **97**, 050404 (2006).
- [15] M. Oshikawa (2010), arXiv:1007.3739.
- [16] B. Hsu and E. Fradkin, *J.Stat.Mech.* **1009**, P09004 (2010).
- [17] M. P. Zaletel, J. H. Bardarson, and J. E. Moore, *Phys.Rev.Lett.* **107**, 020402 (2011).
- [18] J.-M. Stephan, G. Misguich, and V. Pasquier (2011), arXiv:1108.1699.
- [19] A. B. Kallin, M. B. Hastings, R. G. Melko, and R. R. P. Singh, *Phys. Rev. B* **84**, 165134 (2011).
- [20] M. Metlitski and T. Grover, to appear (2011).
- [21] H. Casini and M. Huerta, *Nucl. Phys. B* **764**, 183 (2007).
- [22] M. A. Metlitski, C. A. Fuertes, and S. Sachdev, *Phys. Rev. B* **80**, 115122 (2009).
- [23] S. Ryu and T. Takayanagi, *Phys. Rev. Lett.* **96**, 181602 (2006).
- [24] Y. Zhang, T. Grover, and A. Vishwanath, *Phys. Rev. Lett.* **107**, 067202 (2011).
- [25] A. W. Sandvik, *Phys. Rev. Lett.* **95**, 207203 (2005).
- [26] A. F. Albuquerque and F. Alet, *Phys. Rev. B* **82**, 180408 (2010).
- [27] Y. Tang, A. W. Sandvik, and C. L. Henley, *Phys. Rev. B* **84**, 174427 (2011).
- [28] A. W. Sandvik and H. G. Evertz, *Phys. Rev. B* **82**, 024407 (2010).
- [29] J. Cano and P. Fendley, *Phys. Rev. Lett.* **105**, 067205 (2010).
- [30] S. Isakov, M. B. Hastings, and R. G. Melko, *Nature Physics* **7**, 772 (2011).
- [31] A. Zamolodchikov, *JETP Lett.* **43**, 731 (1986).
- [32] R. C. Myers and A. Sinha, *Phys. Rev. D* **82**, 046006 (2010).
- [33] J. L. Cardy, *Phys. Lett. B* **215**, 749 (1988).
- [34] Z. Komargodski and A. Schwimmer (2011), arXiv:1107.3987.